Int J Biometeorol (2016) 60:361–372
DOI 10.1007/s00484-015-1033-7

ORIGINAL PAPER

Tree-ring-based drought reconstruction in the Iberian Range (east of Spain) since 1694

Ernesto Tejedor[1] · **Martín de Luis**[1] · **José María Cuadrat**[1] · **Jan Esper**[2] · **Miguel Ángel Saz**[1]

Received: 12 February 2015 / Revised: 26 June 2015 / Accepted: 27 June 2015 / Published online: 1 August 2015

Abstract Droughts are a recurrent phenomenon in the Mediterranean basin with negative consequences for society, economic activities, and natural systems. Nevertheless, the study of drought recurrence and severity in Spain has been limited so far due to the relatively short instrumental period. In this work, we present a reconstruction of the standardized precipitation index (SPI) for the Iberian Range. Growth variations and climatic signals within the network are assessed developing a correlation matrix and the data combined to a single chronology integrating 336 samples from 169 trees of five different pine species distributed throughout the province of Teruel. The new chronology, calibrated against regional instrumental climatic data, shows a high and stable correlation with the July SPI integrating moisture conditions over 12 months forming the basis for a 318-year drought reconstruction. The climate signal contained in this reconstruction is highly significant ($p<0.05$) and spatially robust over the interior areas of Spain located above 1000 meters above sea level (masl). According to our SPI reconstruction, seven substantially dry and five wet periods are identified since the late seventeenth century considering ≥±1.76 standard deviations. Besides these, 36 drought and 28 pluvial years were identified. Some of these years, such as 1725, 1741, 1803, and 1879, are also revealed in other drought reconstructions in Romania and Turkey, suggesting that coherent larger-scale synoptic patterns drove these extreme deviations. Since regional drought deviations are also retained in historical documents, the tree-ring-based reconstruction presented here will allow us to cross-validate drought frequency and magnitude in a highly vulnerable region.

Keywords Dendroclimatology · Drought · SPI · Reconstruction · Iberian Range · Spain

✉ Ernesto Tejedor
etejedor@unizar.es

[1] Department of Geography, University of Zaragoza, 50009 Zaragoza, Spain

[2] Department of Geography, Johannes Gutenberg University, 55099 Mainz, Germany

Introduction

Nowadays, there is a high consensus on the possible increase of the average temperature of the planet in upcoming decades. However, such a trend is less evident in precipitation. A probable decline in precipitation and an increase in the frequency and magnitude of droughts have been predicted for the Mediterranean basin even though the uncertainty in predictions about precipitation trends is still high (IPCC 2013).

Several studies analyzing the instrumental data from Spain suggest that drought severity has increased over the past five decades (Vicente-Serrano et al. 2011, 2014). However, the relative short observational data make it difficult to determine changes in drought severity (Redmond 2002) resulting in low confidence in drought trends worldwide (Seneviratne et al. 2012). Despite of major recent efforts, knowledge of droughts affecting the Iberian Peninsula is severely limited due to the fact that most of the historical instrumental climatic records do not begin until the 1950s (Gonzalez-Hidalgo et al. 2011).

The temperature and precipitation dynamics of central and northern Europe are particularly well known due to the paleoclimatic reconstructions of the last millennium (Büntgen et al. 2005; Pauling et al. 2006; Büntgen et al. 2011; Esper et al. 2012 for N-Europe). In southern Europe, recent efforts have increased knowledge on temperature dynamics particularly in

the western Mediterranean region (Creus and Puigdefábregas 1982; Büntgen et al. 2008; Dorado-Liñan et al. 2014). However, paleoclimatic reconstructions of precipitation and drought variability are less frequent (see Rodrigo et al. 1999 and Esper et al. 2014 as exceptions).

In Spain, precipitation has recently been considered as the most important climate element directly affecting human society (water availability, human consumption, political and social stability), economic activities (location of dams, water planning, irrigation, demand by industry), and natural systems (water stress, fires, erosion) (de Castro et al. 2005; Randall et al. 2007 in IPCC 2007). Improving knowledge on how drought frequency and intensity have changed over the last few centuries is, therefore, critically important to evaluate the recent trends, validate future scenarios, and adapt to projected climate change (IPCC 2007, 2013).

Drought is a complex phenomenon, which has led to several indices being defined for its study. The Palmer index of drought severity (PDSI) is based on recent precipitation and temperature in terms of a supply and demand model of soil moisture (Palmer 1965). Some of the problems of the PDSI were solved by development of the self-calibrated PDSI (sc-PDSI) (Wells et al. 2004), which makes it spatially comparable and reports extreme wet and dry events. However, the main problem of the PDSI is related to its fixed scale (between 9 and 12 months), and an autoregressive characteristics whereby index values are affected by the conditions up to 4 years in the past (Guttman 1998). Three reconstructions of the PDSI have been developed for Europe (Esper et al. 2007; Nicault et al. 2008; Esper et al. 2014). The standardized precipitation index (SPI) is based on monthly precipitation data and the cumulative probability of a given rainfall event occurring at a station (McKee et al. 1993). This inbuilt memory supports estimates of the cumulative effects of regional drought. Two SPI reconstructions have been developed for Europe (in Turkey, Touchan et al. 2005; in Romania, Levanic et al. 2013). Finally, there is the standardized precipitation and evapotranspiration index (SPEI), which is based on the same terms as the SPI but includes a temperature component in terms of evapotranspiration in the equation (Vicente-Serrano et al. 2010). Both SPI and SPEI have been recognized as effective indices for identifying dry and pluvial periods in the Mediterranean pine forests (Pasho et al. 2011; Camarero et al. 2013).

The aim of this work is to develop for the first time a dendroclimatic reconstruction of the SPI index using a dense multi-species dendrochronological network from the Iberian Range. Through the SPI reconstruction, we identify and discuss the main drought events occurring in the study area over the last 318 years.

Materials and methods

Site description

We compiled a tree ring network from 21 different locations in the eastern Iberian Range of the Iberian Peninsula (Table 1). The Iberian Range is a southeast oriented mountain system between the Ebro depression and the central plateau. It includes a sequence of hills and depressions with diverse lithology, often isolated, or linked through plateaus. Most of the 21 sites used in this study are from higher-elevation sites, since these are the areas where forests have been least exploited and the oldest trees are located (Fig. 1). The altitude of the sampling sites ranges from 1100 to 2000 meters above sea level (masl), with a mean of 1600 m. The higher-elevation trees belong to the oro-Mediterranean bioclimatic belt characterized by large seasonal temperature fluctuations including frequent frosts in winter (ocassionally reaching −20 °C) and heat exceeding 30 °C during the dry summer period (Fig. 2, data from the Spanish Meteorological Agency). The mean annual precipitation is 520 mm and reaches a maximum during spring and a minimum during winter. It is also worth noting that there are frequent storms during the months of June, July, and August.

Forest composition in the Iberian Range is dominated by pinaceaes, and their wide distribution is determined by plasticity and adaptation to various bioclimatic conditions. Therefore, at lower altitudes, *Pinus halepensis*, associated with typical Mediterranean conditions, are found, while with increasing altitude, *Pinus nigra* and *Pinus sylvestris* represent the dominant tree species. The highest elevations are covered by *Pinus uncinata* reaching its southern distribution limits in the Iberian Range.

Tree ring chronology development

Overall, a total of 336 samples and 45.648 growth rings from five pine species (*P. sylvestris*, *P. uncinata*, *P. nigra*, *P. halepensis*, and *Pinus pinaster)* were used for the development of a regional ring width chronology. The samples originate from three different sources (see Table 1 for an overview) constituting the largest dendrochronological database for the Iberian Range. The most recent data including 184 samples from nine sites was collected during field campaigns in 2012 and 2013, i.e., the outermost rings are 2011 and 2012, respectively. Old dominant and co-dominant trees with healthy trunks with no sign of human intervention (e.g., resin collection) or geomorphological processes were selected at each site. We extracted two core samples from each tree using at breast height (1.3 m) perpendicular to the slope to prevent compression wood. On steep slopes (>15°), the samples were taken at a greater height up to 2 m above ground. Cores were air-dried and glued onto wooden holders and subsequently sanded to ease growth ring identification (Stokes and Smiley

Table 1 Tree ring site characteristics

Code	Site	Source	Lat	Long	Elevation	Species	Tree no.	Sample no.	Tree rings	Period
495	Alcalá de la Selva	ITRDB	40.38	−0.69	1980	*Pinus uncinata*	5	11	1101	1820–1977
BEL	Bellena	IPE-CSIC	40.14	−1.16	1100	*Pinus nigra*	11	22	5843	1584–1993
BES	Castillo de Benatanduz	UNIZAR	40.56	−0.46	1700	*Pinus sylvestris*	11	22	2709	1837–2012
CAH	Camarena de la Sierra	UNIZAR	40.08	−0.99	1600	*Pinus halepensis*	7	14	556	1939–2012
CAS	Camarena de la Sierra	UNIZAR	40.10	−1.00	1800	*Pinus sylvestris*	12	25	4084	1719–2012
E41	Albarracín	ITRDB	40.29	−1.34	1225	*Pinus pinaster*	9	18	2051	1836–1985
E42	Gudar Fuenternarices	ITRDB	40.26	−0.71	1450	*Pinus nigra*	2	4	1078	1681–1984
E43	Gudar Pradillo	ITRDB	40.26	−0.65	1650	*Pinus sylvestris*	3	6	610	1865–1985
E44	Gudar Las Roquetas	ITRDB	40.23	−0.68	1475	*Pinus nigra*	10	21	3199	1681–1985
E46	Gudar Cantavieja	ITRDB	40.55	−0.48	1750	*Pinus sylvestris*	9	18	2100	1844–1985
E47	Gudar Villarluengo	ITRDB	40.36	−0.46	1500	*Pinus nigra*	9	17	2195	1829–1985
E48	Valdecuenca	ITRDB	40.28	−1.44	1550	*Pinus sylvestris*	4	6	535	1891–1985
JAR	Javalambre	IPE-CSIC	40.10	−0.97	1800	*Pinus sylvestris*	9	16	5106	1503–1992
LIN	Mosqueruela	IPE-CSIC	40.37	−0.42	1450	*Pinus nigra*	4	8	1730	1658–1993
PDH	Pinar de Pla	UNIZAR	40.73	0.20	1200	*Pinus halepensis*	4	8	1233	1831–2013
PDS	Pinar de Pla	UNIZAR	40.72	0.18	1250	*Pinus sylvestris*	8	16	1293	1865–2012
PER	Peñarroya	IPE-CSIC	40.38	−0.65	1950	*Pinus uncinata*	3	5	1239	1690–1992
PRS	Peñarroya	UNIZAR	40.39	−0.67	1950	*Pinus sylvestris*	7	13	1664	1830–2011
PRU	Peñarroya	UNIZAR	40.38	−0.67	2000	*Pinus uncinata*	15	30	3303	1711–2011
VAH	Valdecuenca	UNIZAR	40.31	−1.38	1650	*Pinus halepensis*	15	31	2497	1879–2012
VAS	Valdecuenca	UNIZAR	40.30	−1.39	1600	*Pinus sylvestris*	12	25	1522	1916–2012
						Total	169	336	45648	

UNIZAR University of Zaragoza, *IPE-CSIC* Spanish National Research Council, *ITRDB* International Tree-Ring Databank

1968). The cores were scanned and synchronized using the CoRecorder software (Larsson 2012) (Cybis Dendrochronology 2014) to identify the position and exact dating of each ring, and the width measured, at 0.01-mm precision, using a LINTAB table (Rinn 2005). The cross-dating among trees was quality-controlled using the COFECHA program (Holmes 1983).

An additional set of 101 samples from eight sites was downloaded from the International Tree Ring Data Bank (ITRDB, http://www.ncdc.noaa.gov/data-access/paleoclimatology-data/datasets/tree-ring). These data were developed by K. Richter and collaborators in the late 1970s and early 1980s, i.e., the outermost rings range from 1977 to 1984. Another four sites including 51 samples were provided by the project CLI96-1862, i.e., the outermost rings range from 1988 to 1993 (Creus et al. 1992; Genova et al. 1993; Manrique and Fdez. Cancio 2000; Saz 2003).

In order to assess coherence among sampling sites and support averaging tree ring data at the regional scale, a matrix correlation was developed for the common period (1940–1977) and for the full-length period of each site. Then, a mean regional chronology was developed.

For the preservation of interannual to multi-decadal scale variability and in order to eliminate the biological age trend in the radial growth, the 336 individual tree ring width series were standardized using the dplR standardization package (Bunn 2008), executed in Rstudio (R Development Core Team 2014). Each ring width series was fitted with a cubic spline with a 50 % frequency response cutoff at 67 % of the series length (Cook et al. 1990). A first-order autoregressive model of the residuals and a bi-weight robust estimation of the mean (Cook and Peters 1997) were applied to assemble the regional residual chronology (TRI_{res}) for studying the influence of climate on tree growth and reconstructing the main driver at interannual to multi-decadal frequencies.

Chronology confidence was assessed using the express population signal (EPS), and the interseries correlation (Rbar) (Wigley et al. 1984). EPS provides an estimate of how closely a mean chronology based on a finite number of trees matches its hypothetically perfect chronology (Cook et al. 1990). Values equal to or above 0.85 are considered to ensure that a chronology is suitable for climate reconstruction (Wigley et al. 1984). Rbar estimates the common variance among ring width series averaged in a chronology.

Climatic data, calibration, and climate reconstruction

Monthly temperature and precipitation instrumental data (provided by AEMET) from 30 stations within a maximum distance of 50 km, and spanning 1951–2010, were used to

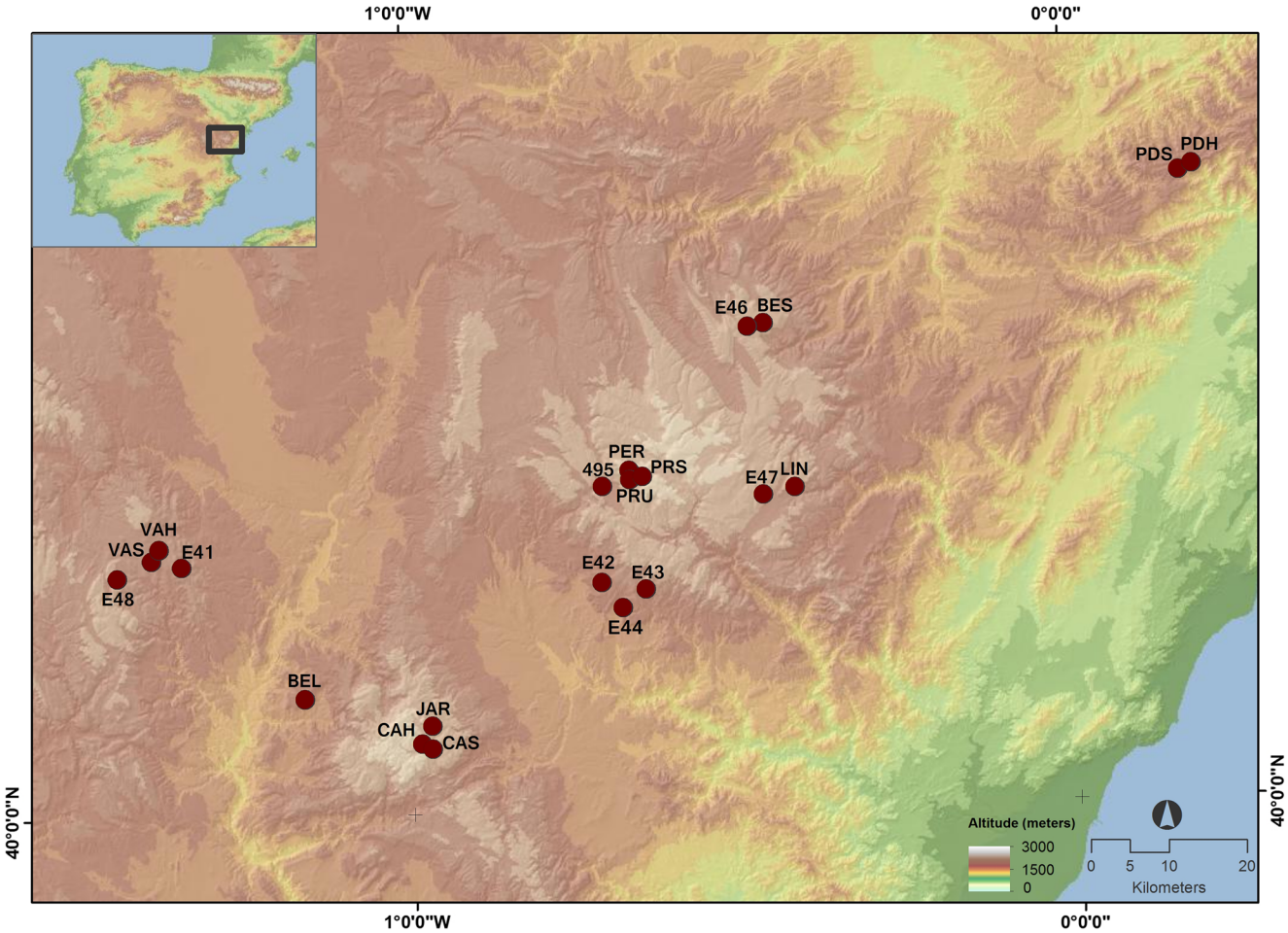

Fig. 1 Map showing the tree ring study sites (*circles*) and city of Teruel in the Iberian Range

calibrate the tree ring data. In addition, gridded instrumental data from CRU TS v.3.22, (1901–2012 period, 0.5° × 0.5° resolution) were used for comparative purposes (Harris et al. 2014). Due to the size of the study area, the average of the three closest grid points was used to construct a regional time series.

Using both station and gridded climate data, we calculated the standardize precipitation index (SPI) and the standardize precipitation-evapotranspiration index (SPEI). The SPI (McKee et al. 1993) is calculated using monthly precipitation as input data while the SPEI (Vicente-Serrano et al. 2010) uses the monthly difference between precipitation and the potential

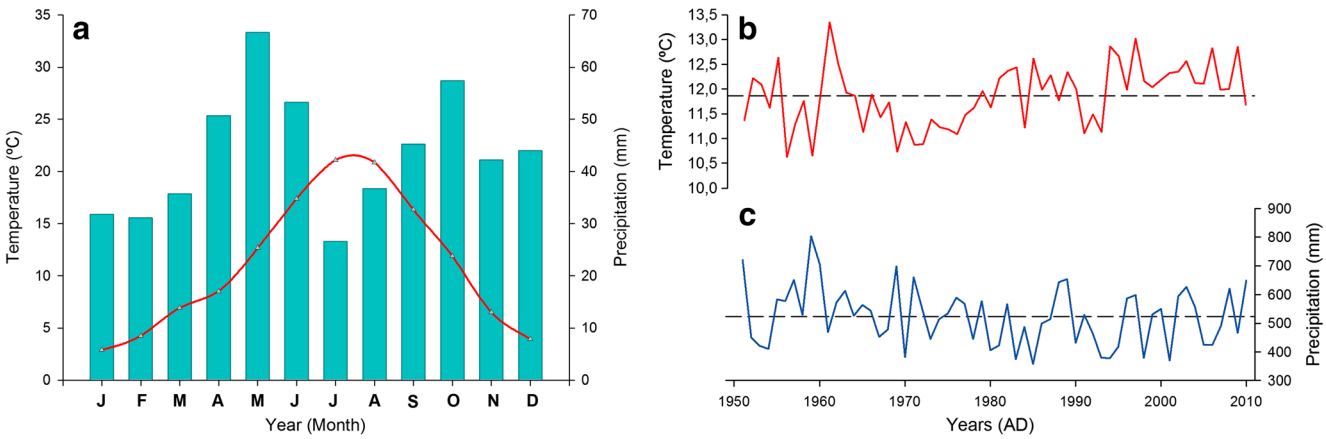

Fig. 2 Climate data. **a** Climate diagram of the study area made from 30 meteorogical stations for the period 1950–2010. **b** Annual temperature, and **c** precipitation from 1950–2010

evapotranspiration. Both indexes were calculated at different time scales from 1 to 24 months for the common period 1951–2010. For calibration, we used the residual chronology (TRI_{res}) to minimize biological memory effects in tree ring width (TRW). Therefore, the high-frequency variability contained in the residual series is expected to be related only with year-to-year climate variability. TRI_{res} was calibrated against the SPI and SPEI for 1 to 24 months using the station-based and gridded climate data.

To evaluate the accuracy of the model used for climate reconstruction, the dataset was split into two equally long periods for calibration and verification (Fritts 1976). These periods were 1951–1980 and 1981–2010. The procedure was then repeated with reversed periods. The consistency of the linear model was tested using the Pearson's correlation coefficient (r), reduction of error (RE), mean square error (MSE), and sign test. RE provides a highly sensitive measure of the reliability of a reconstruction (Akkemik et al. 2005); it ranges from +1, indicating perfect agreement, to minus infinity. Commonly, positive RE values are interpreted as there is some skill in the reconstruction (Fritts et al. 1990). The MSE is an estimate of the difference between the modeled and the measured.

Sign test compares the number of agreeing and disagreeing interval trends, from year to year, between the observed and reconstructed series (Fritts et al. 1990; Cufar et al. 2008).

A linear regression model was used to transfer the residual chronology into a drought index. To identify and evaluate extreme events, we adopted an approach detailed in Akkemik et al. (2005), in which extreme deviations are identified considering standard deviation thresholds. We normalized the reconstruction time series and define extreme dry and wet years considering ≥±1.76 standard deviations (Türkes 1996; Akkemik et al. 2005). An 11-year running mean was applied to identify periodic changes in the reconstruction. The magnitude and spatial extent of the climate signal were assessed considering the gridded CRU TS v.3.22 over the Iberian Peninsula.

Results

Chronology

The correlation matrix with all the sites (Fig. 3) shows the high correlation between sites and species. The high intersite correlations reaching 0.46 from 1940 to 1977 and 0.42 over the full overlapping period justified the development of a 511-year chronology for the eastern Iberian Range covering the 1503–2013 time period (Fig. 4). The highest correlation is found between the highest elevation sites for both *P. uncinata* (PRU and 495) and *P. sylvestris* (PRS and PER) whereas the lowest correlation is found between the lowest *P. halepensis* site (PDH) and the highest *P. sylvestris* site (PER). However, the high mean correlation between sites suggests a common regional climate signal. Therefore, the chronology is based on 336 TRW series of five different *Pinus* spp. The average age of the trees analyzed is 134 years, with a minimum of 20 years and a maximum of 489 years. The mean sensitivity was 0.153, and the first-order autocorrelation for the TRI_{res} was −0.01. The correlation coefficient (Rbar) between trees is 0.29 whereas the correlation within trees equals 0.73. The variance explained by the first principal component is 33.58 % showing that a substantial fraction variability may be due to a single factor. The signal-to-noise ratio reaches 28.09, and EPS exceeds 0.85 after 1694, confining the reconstruction period to 318 years until 2012.

SPI and SPEI signals

The correlations between the residual chronology (TRI_{res}) and the SPI and SPEI indexes from 1 to 24 months from both the regional instrumental series and the CRU regional series for the period 1951–2010 are shown in the Fig. 5. Even though the signal followed a similar pattern with both climate sources, the regional instrumental series always showed higher correlation coefficients (Fig. 5). The most consistent signal was observed for the 10–14-month period centered on July and August ($r>0.6$) for the SPI correlated with the instrumental climate data (Fig. 5b). Correlation coefficients higher than 0.6 are also observed for other particular months and time spans, such as August of SPI4 ($r>0.6$). According to this information, we opted for the $SPI12_{July}$ reconstruction, since this period provides valuable information on a time interval covering a period similar to the full hydrological year and has the highest correlation values ($r=0.63$).

The relationship between the 12-month SPI and the chronology was consistent throughout the eastern Iberian Range (Fig. 6). Correlation values higher than 0.4 extend toward the interior mountain ranges, whereas low correlation values were found in the Ebro depression in the north and in the southern plateau in the southwest.

The reliability of the model was confirmed by the high correlation (0.63) and adjusted correlation coefficients (0.40). The reduction of error (RE) is positive in both calibration and verification periods, indicating that there is skill in the reconstruction (Fritts et al. 1990). MSE and sing test have similar values to those presented in other SPI reconstructions (for instance, Levanic et al. 2013)

The two models obtained for the calibration periods 1951–1980 and 1981–2010 proved to be significantly effective and valid for the final reconstruction (Table 2 and Fig. 7). For the final lineal model, we used the full 1951–2010 period with the station-based SPI12 data (Eq. 1) to develop a SPI reconstruction reaching back to 1694:

$$SPI12_{July} = 4.9381 * TRI_{res} - 5.1132 \left(r^2_{adj} = 0.40; p < 0.01\right) \quad (1)$$

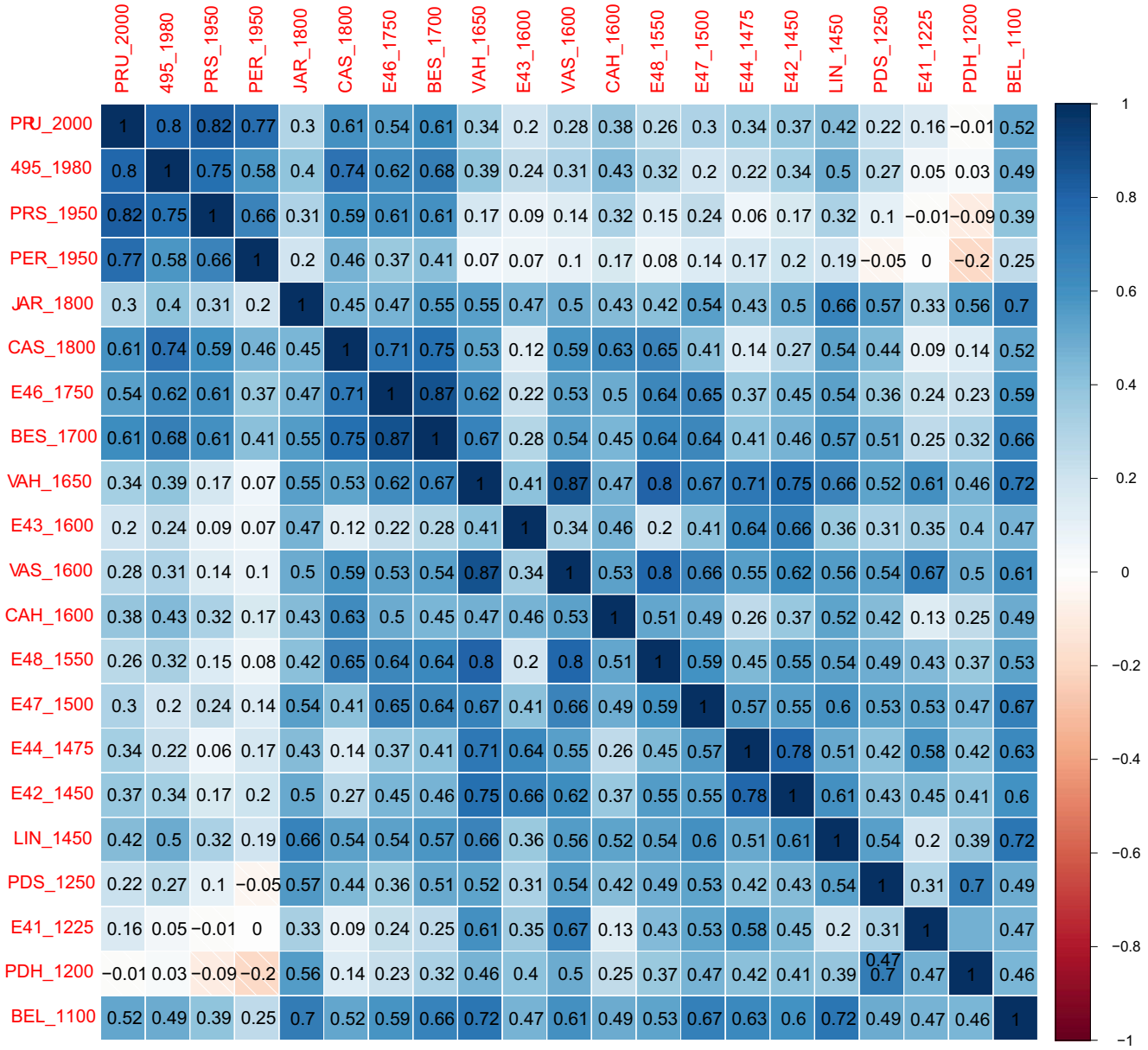

Fig. 3 Correlation of the sampling sites sorted by elevation. *Top right* shows the correlations calculated over the 1940–1977 common period. *Bottom left* shows the correlations over the full periods of overlap between pairs of chronologies

SPI reconstruction

According to reconstruction presented here, the 12 months preceding July 2012 were the driest period with respect to the past 318 years in the Iberian Rang (Table 3). In order to investigate extreme drought and pluvial events, we considered 1.76 standard deviation positive and negative thresholds to identify 36 positive and 28 negative outliers since AD 1694 (Fig. 8). The eighteenth century had a higher recurrence of extreme dry events, whereas it was also the century with the fewest pluvial years. The nineteenth century shows fewer years with extreme events, while the twentieth century contains 38 % of all extreme events. Moreover, 6 of the 10 driest reconstructed years occurred within the last eight decades, and 9 of the 10 wettest reconstructed years occurred over the last 100 years. Concerning the 11-year moving mean, we identified seven dry periods in order of severity (1798–1809, 1961–1972, 1744–1755, 1871–1882, 1981–1992, 1701–1712, and 1771–1782). Accordingly, we identified five wet periods in order of intensity (1949–1960, 1756–1766, 1971–1982,

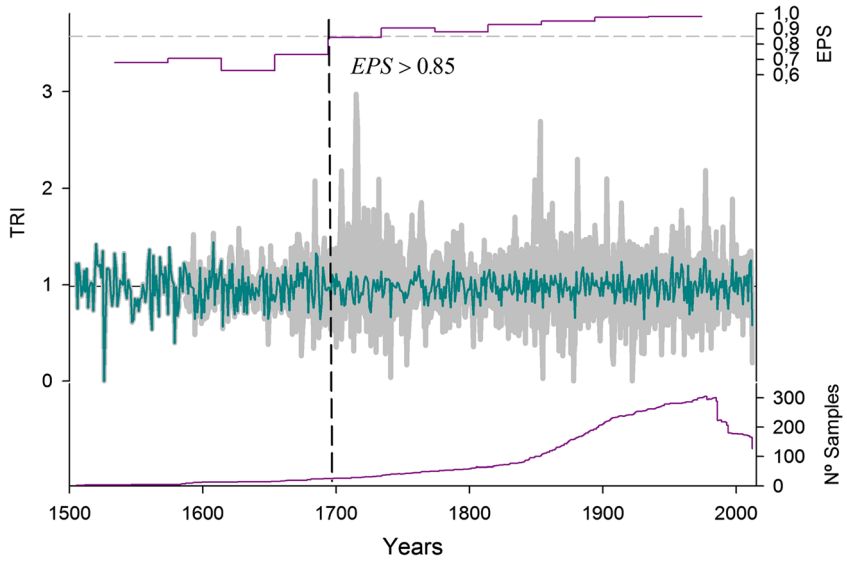

Fig. 4 TRI_{res} chronology (in *green*); the residual chronologies of the 21 sites used (in *gray*); number of samples and EPS (computed over 30-y window lagged by 15 years) threshold in 1694 (Color figure online)

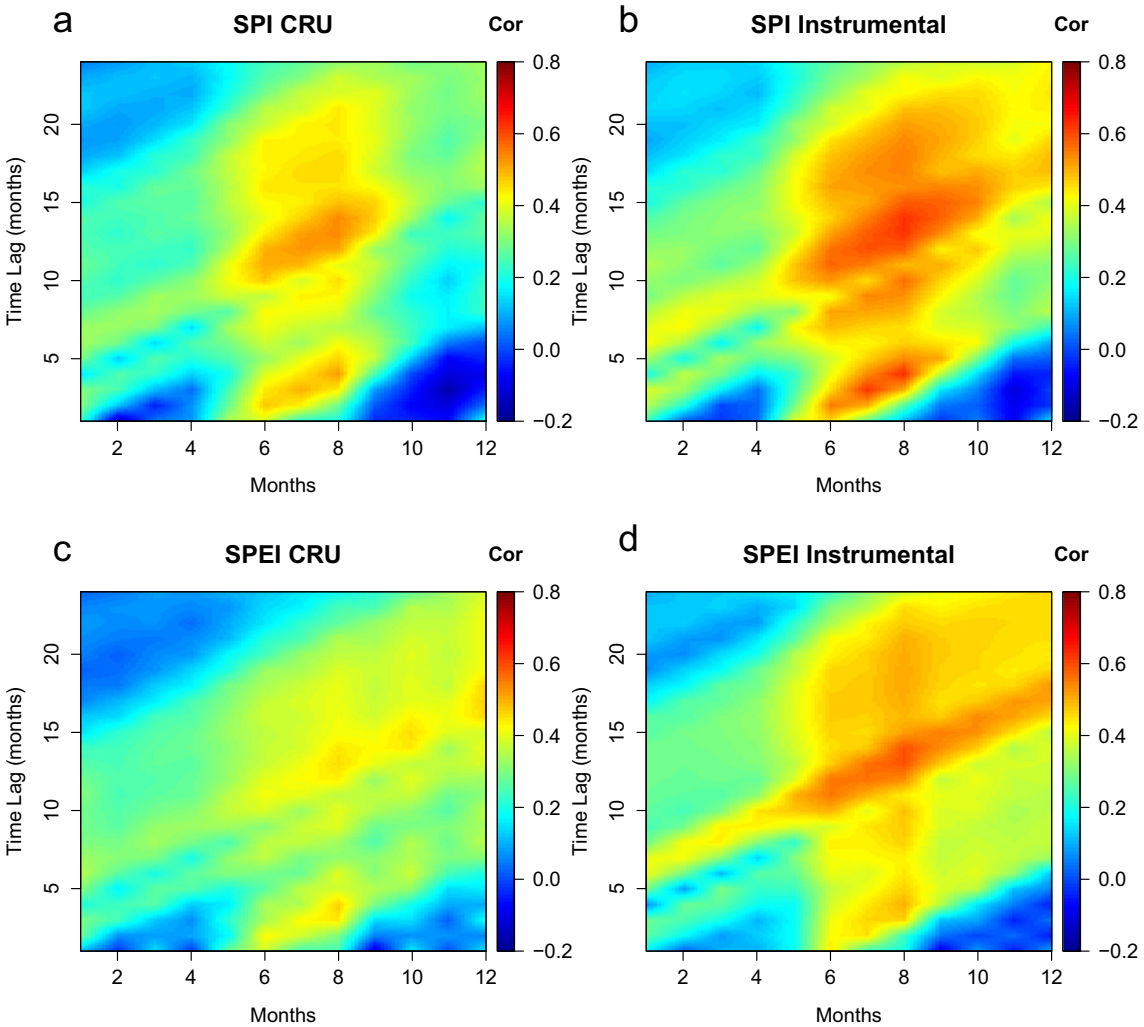

Fig. 5 Correlation between the SPI and SPEI indices for 1 to 24 months and the regional residual chronology. Results for **a**, **c** CRU data and **b**, **d** for station data, both over the period 1951–2010. Correlation values higher than 0.25 are significant at $p<0.05$

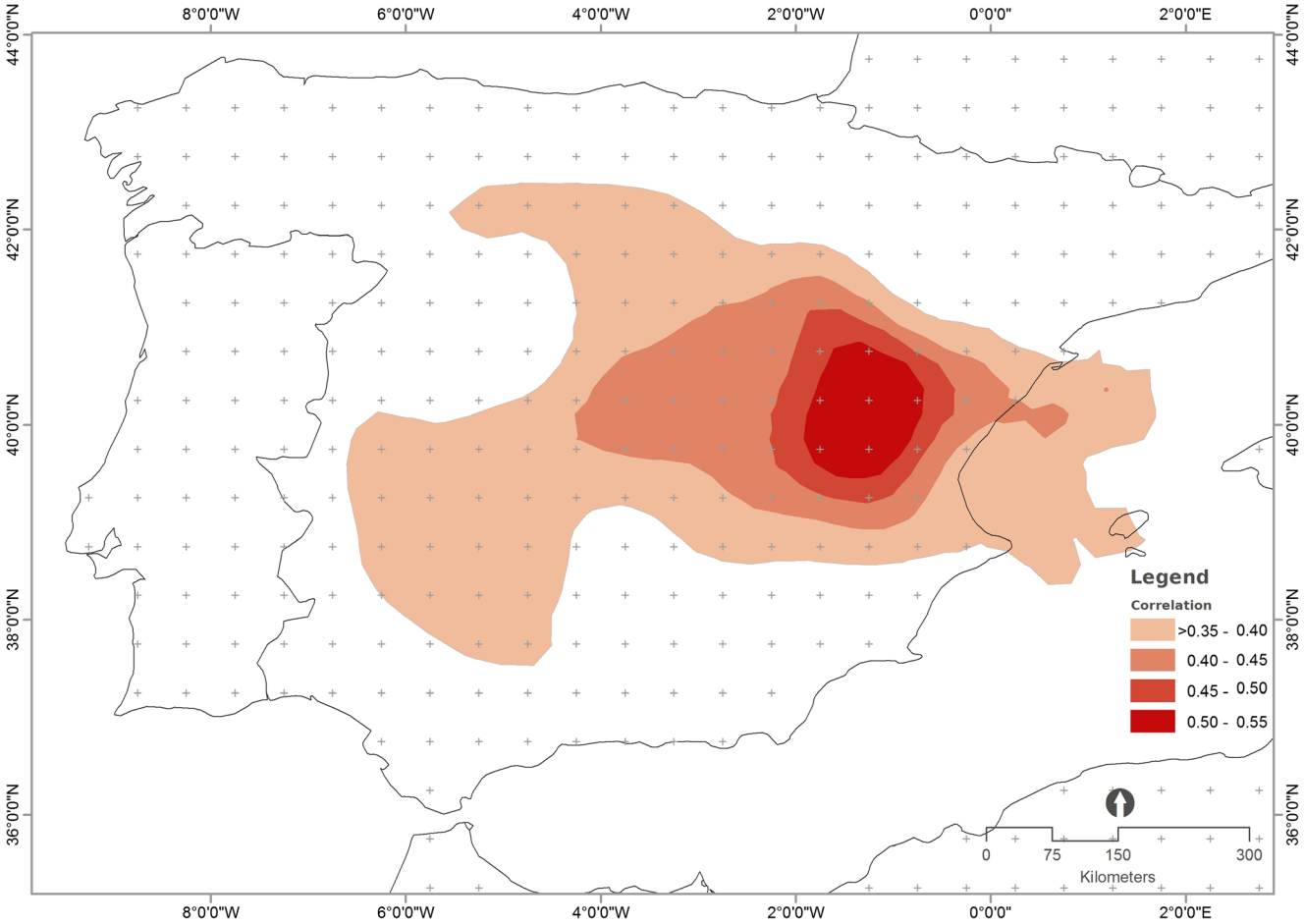

Fig. 6 Spatial correlations for composite TRW chronology with gridded $SPI12_{July}$ data. Correlation values are significant at $p<0.05$

1883–1894, and 1810–1821). The fact that the dry and wet periods are not temporally clustered is to some degree expected after removing low-frequency trends when applying the spline detrending and considering the residual chronology.

Discussion

Paleoclimatic studies show that droughts are a frequent phenomenon throughout the Mediterranean region with vast environmental and socio-economic consequences (Martín-Vide and Vallvé 1995; Rodrigo et al. 1999). Detailed information on these events over the past centuries, particularly during the Little Ice Age (LIA), is scarce, however. Although there are some references regarding long-term precipitation changes (Nesje and Dahl 2003), most studies focused on temperature variability (Büntgen et al. 2013).

Table 2 Calibration/verification statistics $SPI12_{July}$ reconstruction

	Calibration 1951–1980	Verification 1981–2010	Calibration 1981–2010	Verification 1951–1980
Years	30	30	30	30
Correlation	0.55	0.60	0.60	0.55
MSE	0.62	0.73	0.56	0.74
Reduction of error	0.37	0.24	0.46	0.19
Sing test	20+/10−	20+/10−	20+/10−	20+/10−

MSE mean square error

Based on 336 TRW series of 21 sites with a high coherence between species and elevation, we developed a 318-year SPI reconstruction representative for the central region of Spain. The reconstruction is the only record in southern Europe targeting SPI, a drought index integrating monthly precipitation data and the cumulative probability of a given rainfall event occurring at a station (McKee et al. 1993) and useful to characterize extreme dry and wet events. The main statistics used to verify the accuracy of the reconstruction present values similar to existing SPI reconstructions developed for Turkey (Touchan et al. 2005) and Romania (Levanic et al. 2013). For example, the variance explained by the first eigenvector is 33.58 %, while in Turkey, it is 42.75 % and in Romania 44.96 %. The lower percentage of explained variance by the first eigenvector in our composite chronology might be explained by the fact that we used five different *Pinus* species, while in the other reconstructions, only one

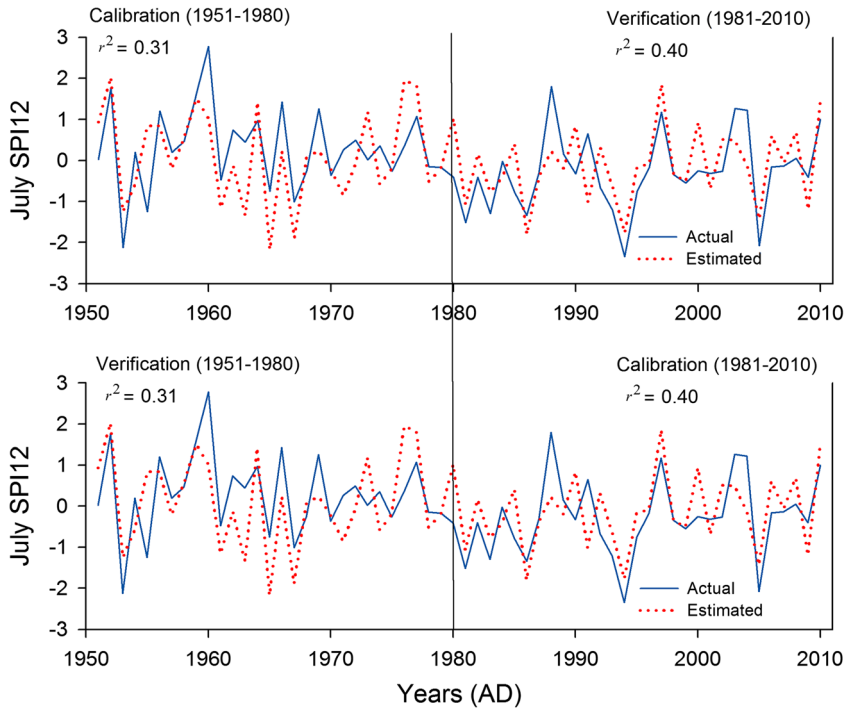

Fig. 7 Calibration and verification results of the station-based $SPI12_{July}$ reconstruction

species was used, *Juniperus excelsa* and *P. nigra*, respectively. The signal-to-noise ratio of 28.09 is higher than that observed by Levanic et al. 2013 (23.03), however.

Table 3 Reconstructed extreme dry and wet years and $SPI12_{July}$ values (in brackets)

	18th Century	19th Century	20th Century	21st Century
Dry extreme events	1704 (−1.47)	1803 (−2.20)	1909 (−1.39)	2005 (−1.43)
	1706 (−1.55)	1808 (−1.53)	1916 (−1.36)	2012 (−2.97)
	1707 (−1.42)	1824 (−1.54)	1924 (−1.47)	
	1713 (−1.32)	1842 (−1.26)	1931 (−2.55)	
	1714 (−1.42)	1849 (−1.32)	1941 (−1.59)	
	1717 (−1.30)	1855 (−1.68)	1953 (−1.25)	
	1725 (−1.63)	1867 (−1.29)	1963 (−1.34)	
	1726 (−2.06)	1879 (−2.44)	1965 (−2.17)	
	1741 (−2.38)		1967 (−1.89)	
	1751 (−1.30)		1986 (−1.80)	
	1766 (−1.47)		1994 (−1.77)	
	1769 (−1.54)			
	1780 (−1.56)			
	1786 (−1.67)			
	1797 (−1.38)			
Wet extreme events	1711 (0.94)	1811 (0.98)	1903 (0.95)	2010 (1.45)
	1734 (0.98)	1815 (1.09)	1914 (1.70)	2011 (1.81)
	1759 (0.94)	1834 (0.99)	1937 (1.05)	
	1762 (1.37)	1846 (1.14)	1940 (1.29)	
	1788 (1.76)	1850 (1.01)	1952 (2.02)	
		1880 (0.94)	1959 (1.51)	
		1885 (1.27)	1960 (1.02)	
			1964 (1.42)	
			1973 (1.18)	
			1976 (1.94)	
			1977 (1.80)	
			1980 (1.01)	
			1997 (1.85)	

The difference between the correlation coefficient (Rbar) between trees (0.29) and the correlation within trees (0.73) is typical for datasets integrating various sites. The mean correlation between sites is 0.46 (Fig. 3) although is higher for the sites above 1800 masl which are *P. uncinata*, *P. sylvestris*, and *P. nigra*. Nevertheless, the mean chronology captures the regional climate signal very well which highlights the advantages of regional averages (Briffa et al. 1998).

The raw chronology was longer than the final reconstruction; however, due to low sample replication, the EPS value drops below 0.85 in the early years of the chronologies (1503–1693). Therefore, the reconstruction was developed for the period 1694–2012. In order to reconstruct droughts for the whole LIA event, more cores of old living trees should be sampled. Additionally, as suggested by Esper et al. (2014), combining the living-tree samples with tree ring width measurements from historical structures would permit extending the reconstruction back in time, perhaps even over the last millennium.

The growth limitations of the *Pinus* sp. in the study area are expressed by the high positive correlation of the TRI_{res} chronology with July SPI integrating drought conditions over 12 months ($SPI12_{July}$). A similar metric was considered by Levanic et al. (2013) in Eastern Europe where the August SPI integrating 3 preceding months was reconstructed. In general, similar responses to late summer precipitation and annual precipitation were detected for other species in the Mediterranean basin (Touchan et al. 2007; Martin-Benito et al. 2010; de Luis et al. 2013).

The high correlation with precipitation is remarkable, since in other mountain areas temperature is usually the limiting factor

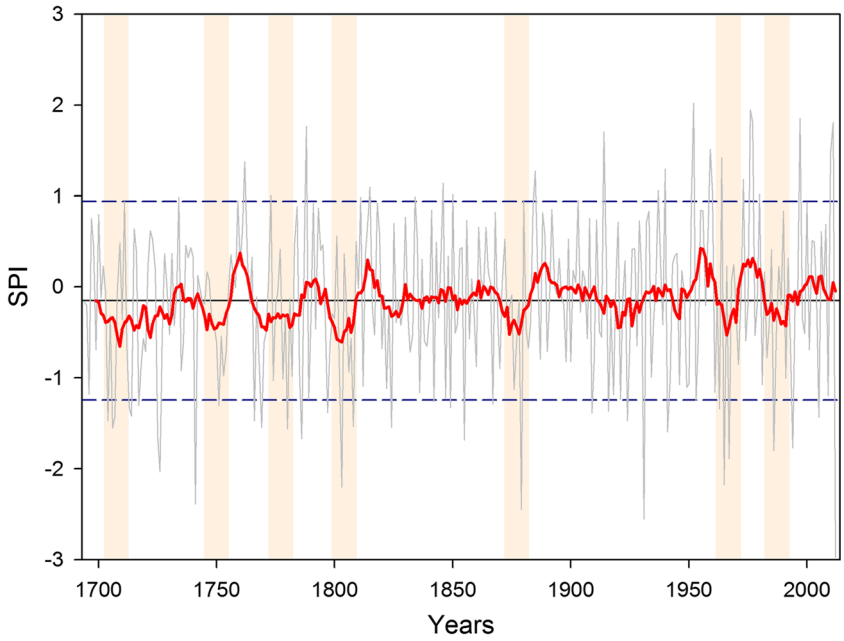

Fig. 8 $SPI12_{July}$ (IRDIR) reconstruction since AD 1694 for the Iberian Range. *Dashed lines* indicate ±1.76 standard deviations used to identify extreme events. *Orange shading* indicates 11-year-long dry periods (Color figure online)

and is commonly used for reconstruction. For instance, in the Alps, TRW has been used to reconstruct temperature (Büntgen et al. 2005), while for the Pyrenees, MXD is needed to get skillful records for a temperature reconstruction (Büntgen et al. 2008). Further south of the IP and with lower-elevation sites than in the Alps and the Pyrenees, we find a strong drought signal.

Our chronology also returned a good correlation with the SPI values on shorter time scales (August SPI for 4 months) and showed the strong influence that late spring and summer precipitation in the study area has on growth of *Pinus* sp. However, the $SPI12_{July}$ correlation is more consistent and not only is reporting information on the complete hydrological year but also is supported by the heavy influence exerted by nutrient storage in the previous year on the following year's growth (Levanic et al. 2013).

With regard to the split calibration/verification approach, we are aware of the limitations of testing the chronology with only 60 years of instrumental data. The general distribution of meteorological observatories in Spain did not begin until the mid-twentieth century, however (Gonzalez-Hidalgo et al. 2011). Thus, even though the CRU dataset covers the 1901–2012 period, for the first 50 years, there were too few instrumental stations to represent the specific climate conditions of the study area. Despite these limitations, the correlation with the calibration period (r^2=0.40) is similar to other precipitation and SPI reconstructions (r^2=0.46, Akkemik et al. 2005; r^2=0.34, Levanic et al. 2013) using a longer time span for calibration.

Throughout this $SPI12_{July}$ reconstruction (IRDIR), we were able to identify droughts and pluvial events over the past 318 years. Drought events were most severe in 2012, 1931, 1879, 1741, 1803, 1965, 1726, 1967, 1986, 1994, and 1725. Some of these years (1803, 1879, 1965, and 1994) are also identified by Genova (2012) as years with severe droughts in Spain. In contrast, extremely wet events occurred in 1952, 1976, 1997, 2011, 1977, 1788, 1914, 1959, 2010, and 1964. Although there is overlap in some extreme dry and wet years with other drought reconstructions developed from other regions of Europe (Akkemik et al. 2005 for 1725, 1726,1797; Esper et al. 2007 for 1803, 1808; Buntgen et al. 2010 for 1959, 1967; Levanic et al. 2013 for 1725, 1914), what is truly remarkable is the consistency of the frequency of extreme events. While in the eighteenth century there was a high frequency of extreme events, in the nineteenth century, the frequency decreased considerably making a very quiet century in terms of droughts which might seem to be related to the end of the LIA (Jones and Bradley, 1992). In the northeast of Spain, the end of this episode does not seem to be related to a temperature increase, but to a decrease in the interannual variability (Saz 2003) and a reduced frequency of extreme drought events (Manrique and Fernández 2000), at least compared to what has been observed in the previous centuries, particularly the sixteenth and seventeenth. However, the frequency of the extreme events increases again during the twentieth century, particularly over the most recent 80 years, which is consistent with the last IPCC report (2013) linking anthropogenic activities with global climate change.

A larger number of extreme events are associated with catastrophic historical and cultural changes over the past 318 years. For instance, the great drought of 1725 (SPI of −1.63) is known as *El año sin cosecha* (the year without a harvest) in Monegros (Alberola 1996). Monegros is located in the north of the study region, which used to be an important bread basket for the Mediterranean population. The year 1725 was also reported to have been an extremely dry year with a

serious famine and poverty in Romania (Levanic et al. 2013). Furthermore, Touchan et al. (2007) described 1725 as "the year with major drought in Anatolia and Syria." The period 1749–1753 was very poor in terms of wheat harvest due to droughts having enormous socio-economic impact.

There are more episodes affecting harvests such as the great famine events during the first decade of the nineteenth century, which is reflected in the IRDIR with two dry extreme events (1803, SPI of −2.20, and 1808, SPI of −1.53). It is well known as the decade of nineteenth-century famines (*Hambres decimonónicas*). In 1803, thousands of people died in northeast Spain due to the lack of wheat brought about by poor harvests. Vicente-Serrano and Cuadrat-Prats (2007) indicated that 1803 was the year with the second highest number of rogations in the nineteenth century in Teruel and Zaragoza. At the end of that century, there was another period of severe famine caused by wheat shortages driving the price up. The year 2012 is described by the Spanish Meteorological Agency (AEMET) as an extremely dry and warm year all over Spain, and one which had socio-economic consequences.

The spatial representation of the IRDIR serves to characterize the climate of inland continental areas of the Iberian Peninsula. The IRDIR is consistent throughout the north and south plateau with a high correlation ($r>0.50$); however, it is not so representative of the great depressions such as the Ebro Valley. The same pattern was presented by Esper et al. (2014), although the PDSI index and *Juniperus* sp. were used. These patterns allow us to identify a biogeographical region covering the entire Iberian Range as well as the central system and the north and south plateau. The area showing high correlations is mostly above 1000 masl (Fig. 6). However, in the main depressions such as the Ebro, the Duero, or the Tajo valleys, the IRDIR is not representative. Climate conditions affecting other high-altitude areas of Spain, such as the Pyrenees and Sierra Nevada, differ in terms of temperature and precipitation; therefore, the IRDIR does not represent these areas either.

Acknowledgments This study was supported by the Spanish government (CGL2011-28255) and the government of Aragon throughout the "Program of research groups" (group Clima, Cambio Global y Sistemas Naturales, BOA 147 of 18-12-2002) and FEDER funds. Ernesto Tejedor is supported by the government of Aragon with a Ph.D. grant. Fieldwork was carried out in the province of Teruel; we are most grateful to its authorities for supporting the sampling campaigns. We are thankful to Klemen Novak, Edurne Martinez, Luis Alberto Longares, and Roberto Serrano for help during fieldwork. We thank Elaine Rowe for improving the English of this manuscript.

References

Akkemik Ü, Dağdeviren N, Aras A (2005) A preliminary reconstruction (A.D. 1635–2000) of spring precipitation using oak tree rings in the western Black Sea region of Turkey. Int J Biometeorol 49(5):297–302

Alberola A (1996) La percepción de la catástrofe: sequía e inundaciones en tierras valencianas durante la primera mitad del siglo XVIII. Revista de Historia Moderna 15:257–299

Briffa KR, Schweingruber FH, Jones PD, Osborn TJ, Shiyatov SG, Vaganov EA (1998) Reduced sensitivity of recent tree-growth to temperature at high northern latitudes. Nature 391:678–682

Bunn AG (2008) A dendrochronology program library in R (dplR). Dendrochronologia 26:115–124

Büntgen U, Esper J, Frank DC, Nicolussi K, Schmidhalter M (2005) A 1052-year tree-ring proxy for alpine summer temperatures. Clim Dyn 25(2–3):141–153

Büntgen U, Frank D, Grudd H, Esper J (2008) Long-term summer temperature variations in the Pyrenees. Clim Dyn 31(6):615–631. doi:10.1007/s00382-008-0390-x

Büntgen U, Brázdil R, Frank D, Esper J (2010) Three centuries of Slovakian drought dynamics. Clim Dyn 35(2):315–329. doi:10.1007/s00382-009-0563-2

Büntgen U, Brázdil R, Dobrovolný P, Trnka M, Kyncl T (2011) Five centuries of Southern Moravian drought variations revealed from living and historic tree rings. Theor Appl Climatol 105(1):167–180. doi:10.1007/s00704-010-0381-9

Büntgen U, Kyncl T, Ginzler C, Jacks DS, Esper J, Tegel W, Heussner KH, Kyncl J (2013) Filling the Eastern European gap in millennium-long temperature reconstructions. Proc Natl Acad Sci U S A 110(5):1773–1778. doi:10.1073/pnas.1211485110

Camarero JJ, Manzanedo RD, Sanchez-Salguero R, Navarro-Cerrillo RM (2013) Growth response to climate and drought change along an aridity gradient in the southernmost *Pinus nigra* relict forests. Ann For Sci 70(8):769–780

Cook ER, Peters K (1997) Calculating unbiased tree-ring indices for the study of climatic and environmental change. The Holocene 7:361–370

Cook ER, Briffa K, Shiyatov S, Mazepa V (1990) Tree-ring standardization and growth trend estimation. In: Cook ER, Kairiukstis LA (eds) Methods of dendrochronology: applications in the environmental sciences. Kluwer Academic Publishers, Dordrecht, pp 104–162

Creus J, Puigdefabregas J (1982) Climatología histórica y dendrocronología de *Pinus uncinata* R. Cuad Investig Geográfica 2(2):17–30

Creus J, Génova M, Fernandez Cancio A, Perez Antelo A (1992) New dendrochronologies for Spanish Mediterranean zone. Lundqua Rep 34:76–78

Čufar K, de Luis M, Eckstein D, Kajfez-Bogataj L (2008) Reconstructing dry and wet summers in SE Slovenia from oak tree-ring series. Int J Biometeorol 52:607–615

De Castro M, Martín-Vide J, Alonso S (2005) El clima de España: pasado, presente y escenarios de clima para el siglo XXI. In: Moreno Rodriguez JM (ed) Evaluación preliminar de los impactos en España por efecto del cambio climático. Ministerio de Medio Ambiente, Madrid, pp 1–65

de Luis M, Cufar K, Di Filippo A, Novak K, Papadopoulos A, Piovesan G, Rathgeber CBK, Raventós Josep, Saz MA, Smith KA (2013) Plasticity in dendroclimatic response across the distribution range of Aleppo pine (Pinus halepensis). PloS One 8(12):e83550

Dorado Liñán I, Zorita E, González-Rouco JF, Heinrich I, Campello F, Muntán E, Andreu-Hayles L, Gutiérrez E (2014) Eight-hundred years of summer temperature variations in the southeast of the Iberian Peninsula reconstructed from tree rings. Clim Dyn 19 p

Esper J, Frank D, Büntgen U, Verstege A, Luterbacher J, Xoplaki E (2007) Long-term drought severity variations in Morocco. Geophys Res Lett 34(17):L17702. doi:10.1029/2007gl030844

Esper J, Frank DC, Timonen M, Zorita E, Wilson RJS, Luterbacher J, Holzkämper S, Fischer N, Wagner S, Nievergelt D, Verstege A, Büntgen U (2012) Orbital forcing of tree-ring data. Nat Clim Chang 2:862–866

Esper J, Großjean J, Camarero JJ, García-Cervigón AI, Olano JM, González-Rouco JF, Domínguez-Castro F, Büntgen U (2014)

Atlantic and Mediterranean synoptic drivers of central Spanish juniper growth. Theor Appl Climatol
Fritts HC (1976) Tree rings and climate. Academic Press, London
Fritts HC, Guiot J, Gordon GA, Schweingruber FH (1990) Methods of calibration, verification, and reconstruction. In Methods of Dendrocrhonology
Génova M (2012) Extreme pointer years in tree-ring records of Central Spain as evidence of climatic events and the eruption of the Huaynaputina Volcano (Peru, 1600 AD). Clim Past 8(2):751–764
Génova M, Fernández Cancio A, Creus J (1993) Diez series medias de anillos de crecimiento en los sistemas Carpetano e Ibérico. Investigación agraria. Sistemas y Recursos Forestales 2:151–172
Gonzalez-Hidalgo JC, Brunetti M, de Luis M (2011) A new tool for monthly precipitation analysis in Spain: MOPREDAS database (monthly precipitation trends December 1945–November 2005). Int J Climatol 31:715–731
Guttman NB (1998) Comparing the palmer drought index and the standardized precipitation index. J Am Water Resour Assoc 34:113–121. doi:10.1111/j.1752-1688.1998.tb05964.x
Harris I, Jones PD, Osborn TJ, Lister DH (2014) Updated high-resolution grids of monthly climatic observations - the CRU TS3.10 Dataset. Int J Climatol 34(3):623–642
Holmes RL (1983) Computer-assisted quality control in tree-ring dating and measurement. Tree-Ring Bull 43:69–78
IPCC (2007) In: Solomon S, Qin D, Manning M et al (eds) Climate change 2007: the physical science basis. Contribution of working group I to the fourth assessment report of the intergovernmental panel on climate change. Cambridge University Press, Cambridge, p 996
IPCC (2013) Climate change 2013: the physical science basis. Contribution of working group i to the fifth assessment report of the intergovernmental panel on climate change [Stocker, T.F., D. Qin, G.-K. Plattner, M. Tignor, S.K. Allen, J. Boschung, A. Nauels, Y. Xia, V. Bex and P.M. Midgley (eds.)]. Cambridge University Press, Cambridge, United Kingdom and New York, NY, USA, 1535 pp, doi:10.1017/CBO9781107415324
Jones PD, Bradley RS (1992) Climatic variations over the last 500 years. In: Bradley RS, Jones PD (eds) Climate since AD 1500. Routledge, London and New York, pp 649–65
Larsson LA (2012) CoRecorder&CDendro program. Cybis Elektronik & Data AB. Version 7.6
Levanič T, Popa I, Poljanšek S, Nechita C (2013) A 323-year long reconstruction of drought for SW Romania based on black pine (Pinus Nigra) tree-ring widths. Int J Biometeorol 57(5):703–714
Manrique E, Fernandez-Cancio A (2000) Extreme climatic events in dendroclimatic reconstructions from Spain. Clim Chang 44(1–2): 123–138
Martín-Benito D, Del Río M, Cañellas I (2010) Black pine (Pinus nigra Arn.) growth divergence along a latitudinal gradient in Western Mediterranean mountains. Annals of Forest Science, 67 (4)
Martín-Vide J, Vallvé MB (1995) The use of rogation ceremony records in climatic reconstruction: a case study from Catalonia (Spain). Clim Chang 30(2):201–221
McKee TB, Doesken NJ, Kliest J (1993) The relationship of drought frequency and duration to time scales. In: Proceedings of the 8th Conference on Applied Climatology, Anaheim, CA, USA, 17–22. American Meteorological Society, Boston, MA, USA, pp 179–184
Nesje A, Dahl SO (2003) The 'Little Ice Age' - Only temperature? The Holocene 13(1):139–145
Nicault A, Alleaume S, Brewer S, Carrer M, Nola P, Guiot J (2008) Mediterranean drought fluctuation during the last 500 years based on tree-ring data. Clim Dyn 31(2):227–245. doi:10.1007/s00382-007-0349-3
Palmer WC (1965) Meteorological drought. Research Paper 45, US Dept. Commerce, Washington
Pasho E, Camarero JJ, de Luis M, Vicente-Serrano SM (2011) Impacts of drought at different time scales on forest growth across a wide climatic gradient in north-eastern Spain. Agric For Meteorol 151(12): 1800–1811
Pauling A, Luterbacher J, Casty C, Wanner H (2006) Five hundred years of gridded high-resolution precipitation reconstructions over Europe and the connection to large-scale circulation. Clim Dyn 26(4):387–405. doi:10.1007/s00382-005-0090-8
R Core Team (2014) R: a language and environment for statistical computing. R Foundation for Statistical Computing, Vienna, Austria. URL http://www.R-project.org/
Randall DA, Wood RA et al (2007) Climate models and their evaluation. In: Climate change 2007: the physical science basis. Contribution of working group I to the fourth assessment report of the intergovernmental panel on climate change [Solomon S et al (eds)]. Cambridge University Press, Cambridge, UK and New York, NY
Redmond KT (2002) The depiction of drought Bull. Am Meteorol Soc 83:1143–1147
Rinn F (2005) TSAPWinTM – Time series analysis and presentation for dendrochronology and related applications, Version 4.69
Rodrigo FS, Esteban-Parra MJ, Pozo-Vázquez D, Castro-Díez Y (1999) A 500-year precipitation record in Southern Spain. Int J Climatol 19(11):1233–1253
Saz MA (2003) Análisis de la evolución del clima en la mitad septentrional de España desde el siglo XV a partir de series dendroclimáticas. Servicio de Publicaciones de la Universidad de Zaragoza, Zaragoza, **1105 pp**
Seneviratne SI et al (2012) Changes in climate extremes and their impacts on the natural physical environment IPCC special report: managing the risks of extreme events and disasters to advance climate change adaptation ed CB Field et al. (Cambridge: Cambridge University Press) pp 109–230
Stokes MA, Smiley TL (1968) An introduction to tree-ring dating, 2nd edn. The University of Arizona Press, Tucson
Touchan R, Funkhouser G, Hughes M, Erkan N (2005) Standardized precipitation index reconstructed from Turkish tree-ring widths. Clim Chang 72(3):339–353. doi:10.1007/s10584-005-5358-9
Touchan R, Akkemik Ü, Hughes MK, Erkan N (2007) May-June precipitation reconstruction of southwestern Anatolia, Turkey during the last 900 years from tree rings. Quat Res 68(2):196–202
Türkes M (1996) Meteorological drought in Turkey: a historical perspective. 1930–93. Drought Netw News 8:17–21
Vicente-Serrano SM, Beguería S, López-Moreno JI (2010) A multiscalar drought index sensitive to global warming: the standardized precipitation evapotranspiration index. J Clim 23(7):1696–1718
Vicente-Serrano SM, Cuadrat-Prats JM (2007) Trends in drought intensity and variability in the Middle Ebro Valley (NE Spain) during the second half of the twentieth century. Theor Appl Climatol 88:247–258
Vicente-Serrano SM, López-Moreno JI, Beguería S, Lorenzo-Lacruz J, Morán E, Azorín-Molina C (2011) Effects of warming processes on droughts and water resources in the NW Iberian Peninsula (1930–2006). Clim Res 31:2102–2114
Vicente-Serrano SM, Lopez-Moreno JI, Beguería S, Lorenzo-Lacruz J, Sanchez-Lorenzo A, García Ruiz JM, Azorin-Molina C, Morán-Tejeda E, Revuelto J, Trigo R, Coelho F, Espejo F (2014) Evidence of increasing drought severity caused by temperature rise in southern Europe. Environ Res Lett 9 (4), art. no. 044001
Wells N, Goddard S, Hayes MJ (2004) A self-calibrating palmer drought severity index. J Clim 17:2335–2351
Wigley TML, Briffa K, Jones PD (1984) On the average value of correlated time series, with applications in dendroclimatology and hydrometeorology. J Clim Appl Meteorol 23:201–213